Scratch-Resistant Hydrophobic Coating with Supramolecular-Polymer Co-Assembly

Pin-Wei Lee, Adrian Saura-Sanmartin, and Christoph A. Schalley*

Supramolecular assembly for superhydrophobic coatings is known for its efficiency and efficacy. However, the mechanical fragility of the coatings limits their use as coating materials. Herein, the combination of (±)-*N,N'*-(*trans*-cyclohexane-1,2-diyl)-bis(perfluorooctanamide) CF7, a cyclohexyl diamide-based low molecular weight gelator, with acrylate polymers for the generation of semi-transparent omniphobic coatings with significantly enhanced scratch proofness is presented. CF7 has shown the ability to self-assemble in common solvents into highly entangled fibrous networks with extreme water repellency. The incorporation of covalent polymers, specifically poly(methyl methacrylate) (PMMA) and poly(trifluoroethyl methacrylate) (PTFEMA), helps to fixate the supramolecular CF7 fibers without interfering with the self-assembled structures. The resulting coatings, namely CF7/PMMA and CF7/PTFEMA, show significantly improved mechanical resistance as well as optical transparency while maintaining excellent water and oil repellency. Furthermore, the homogeneity of the coating in bulk is confirmed by depth profiling of the 3D distribution of the components using time-of-flight secondary ion mass spectrometry imaging, which turns out to be an essential technique in order to characterize such materials.

1. Introduction

Low molecular weight gelators (LMWGs) are materials of great interest due to their versatility and ease of fabrication.[1–8] Furthermore, these materials are postulated as ideal scaffolds for different applications in catalysis,[9–11] bioengineering,[12–16] and materials science,[17–19] among others, due to the tailorable properties and functions that can be obtained through a rational design.

The use of LMWGs as coating materials offers advantages, such as low cost, short curing time, and scalability. However, one major disadvantage of LMWGs is their mechanical fragility. Thus, applications where the coating needs to withstand mechanical stress or abrasion are limited by this drawback. To overcome this limitation, researchers have tried to change the design of the gelator and equipped it with polymerizable groups like acrylic esters, acrylic amides and diacetylene,[20–23] used metal coordination,[24,25], or added commercially available polymers.[26,27]

Polymer coatings, on the other hand, are highly resistant to abrasion. Excellent mechanical properties make them an attractive alternative to LMWG coatings, especially in applications where durability is a critical factor. One of the primary drawbacks of polymer coatings is that they usually have moderate water repellency compared to LMWG coatings, although some exceptions of functionalized polymer coatings have been reported with high water contact angles and low sliding angles.[28,29] Creating surface roughness on the polymers is one of the most popular solutions to enhance the hydrophobicity, but often involves nanoparticles[30–32] or requires elaborate protocols like lithography, chemical etching, or plasma treatment.[33–38]

In our previous study of superhydrophobic xerogel coatings made from (±)-*N,N'*-(*trans*-cyclohexane-1,2-diyl)-bis(perfluorooctanamide) (**CF7**),[39–41] we found the coating to be quite resistant to intense water flows, since after five cycles of flushing 4 L of deionized water to the xerogel over a minute, the water contact angle (WCA) values hardly decreased (from 153° ± 3° to 150° ± 6°). However, gravimetric analyses indicated a loss of around 13% of the deposited material after these five flushing cycles. Therefore, we decided to conduct further studies toward the preparation of more resistant materials. En route to prepare such improved coatings, the deposition of our **CF7**-based xerogel coatings together with a stabilizing covalent polymer should provide materials with improved iterability and longer lifespans, which is essential to waterproof materials that need

P.-W. Lee, A. Saura-Sanmartin, C. A. Schalley
Institut für Chemie und Biochemie
Freie Universität Berlin
Arnimallee 20, 14195 Berlin, Germany
E-mail: c.schalley@fu-berlin.de
A. Saura-Sanmartin
Departamento de Química Orgánica
Facultad de Química
Campus de Espinardo
Universidad de Murcia
Murcia 30100, Spain

2309140 (1 of 8)

**ADVANCED
SCIENCE NEWS**

www.advancedsciencenews.com

**ADVANCED
FUNCTIONAL
MATERIALS**

www.afm-journal.de

to be exposed to more abrasive conditions. In 1996, Gankema et al. demonstrated the first example of embedding xerogel networks inside a polymer matrix.[42] Monomers and crosslinking reagents that are UV curable are used as solvents in the organogel system to create the aggregates-embedded resin. The aggregates can be later removed to provide nanostructured porous polymeric materials.[43–45] The groups of Stupp,[46,47] Kostopoulus,[48] and Korley[49] have reported the toughening of polymers using supramolecular polymers or gels. In addition, the composition of organogelators and polymerizable components used particularly in dental composite to reduce shrinkage and/or to improve mechanical properties have been reported.[50,51] However, to the best of our knowledge, no examples of fixating a xerogel network with polymers for a more durable hydrophobic coating have been reported.

Here, we report the combination of polymers and LMWG in superhydrophobic coatings with improved mechanical stability. Acrylate monomers are considered for their availability, variety, and the ease of curing. Simple acrylate monomers, like methyl acrylate and methyl methacrylate (MMA), are very common in industrial applications. One of the most appealing features about these monomers is that they can undergo photopolymerization without complicated setup. The fabrication can be done with low power bench-top UV chambers and can be scaled up easily. Although a decrease in the value of WCAs is expected, a significant enhancement of the mechanical resistance is envisioned due to the robustness provided by the polymeric matrix. For this work, MMA was chosen for the polymer's exceptional mechanical properties and low cost. In addition, trifluoroethyl methacrylate (TFEMA) was included in order to investigate the effect of a fluorine-containing monomer in the mixture with fluorinated gelators. The microstructure of the supramolecular-polymer co-assembly was examined with scanning electron microscopy (SEM). X-Ray photoelectron spectroscopy (XPS) was used to characterize the outer surface of the coatings. Furthermore, imaging and depth profiling with time-of-flight secondary ion mass spectrometry (ToF-SIMS) were used to investigate the uniformity of the co-assembly coating. The iterability of the coating was tested by repeating water flushing.

2. Results and Discussion

2.1. Coating Characterization

The supramolecular-polymer coatings, namely **CF7/PMMA** and **CF7/PTFEMA**, are prepared by mixing the corresponding monomer with the organogel of **CF7**,[39] treating the mixture with UVA for a short time, and then applying the mixture to the substrate before final curing. In order to achieve homogeneity of the coating, the irradiation time before drop casting is crucial. Insufficient time will lead to phase separation between the organogel and the monomer/polymer phase, while excessive time will cause the mixture to be overly viscous, resulting in considerably thick filaments in the co-assembly that reduce surface roughness. This irradiation time will differ between the choice of monomer, the photoinitiator, and its concentration.

The morphology of **CF7/PMMA** and **CF7/PTFEMA** coatings was examined by SEM, showing that both materials retain the fibrous network obtained from the pristine **CF7** xerogels throughout the surface (**Figure 1**). Consequently, the presence of the monomer did not disturb the formation of the fibrous network of **CF7**. Moreover, the presence of fluorine on the outer surface of both co-assemblies was confirmed with XPS analysis (see Supporting Information).

The uniform distribution of **CF7** and PMMA or PTFEMA throughout the surface of the coatings was confirmed by the reconstruction of the 3D distribution of **CF7/PMMA** and **CF7/PTFEMA** coating samples using ToF-SIMS. While sputtering using a 5 kev Ar^+_{2000} cluster ion beam allowed to record the spectrometric data of the **CF7** coating, both co-assemblies required to increase the energy of the cluster ion beam to 20 kev in order to carry out such analysis. This observation already indicates a higher coating robustness caused by the presence of a polymeric matrix in the xerogel coatings. ToF-SIMS imaging together with depth profiling suggest a thin layer of material in the pristine **CF7** xerogel coating (**Figure 2**a), while the thickness increases in those samples having polymers (Figure 2b,c). Ions with m/z value of 906.04 attributed to **CF7** were detected in all the samples (see Figures S1– S3, Supporting Information). Additional ions having m/z values of $n*100.05$ and $n*154.02$ (where $n = 1, 2, 3, 4, 5...$) for different fragments of PMMA and PTFEMA, respectively, were also detected throughout the **CF7/PMMA** and **CF7/PTFEMA** coatings (see Figures S2 and S3, Supporting Information), thus confirming the desired uniform distribution which would result in the envisioned hydrophobic properties and high mechanical resistance.

Fourier transform infrared (FT-IR) analyses shows shifts of several PMMA and PTFEMA bands for the **CF7/PMMA** and **CF7/PTFEMA** coatings (see Figures S4– S8, Supporting Information), highlighting those related to sp³ C-H and ester C=O stretching. The amide C=O stretching band of **CF7** also experiences a shifting in both co-assemblies, thus suggesting interactions between the components of the aggregates.

2.2. Contact Angles

The hydrophobicity of the coatings was tested by the measurement of the WCAs. As above mentioned, coatings made from **CF7**-based xerogels turned out to be superhydrophobic, showing a WCA of 153° ± 3° (**Table 1**, entry 1). The coatings of the co-assemblies show slight decreases in the WCA values as expected, due to the homogeneous distribution of polymer and **CF7**, which leads to a smaller fluorinated surface area. Thus, the WCA decreases by 2.6% (WCA 149°) in the **CF7/PMMA** coating (Table 1, entry 2) and by 9.8% (WCA 138°) in the **CF7/PTFEMA** coating (Table 1, entry 3). This difference between both polymer-bearing coatings can be attributed to the distinct morphology of the surfaces. Possible nanostructures are visible in the **CF7/PMMA** co-assembly (see Figure S9, Supporting Information), while they are not found in the **CF7/PTFEMA** co-assembly. These nanostructures could lead to an enhancement in the WCAs of **CF7/PMMA**. The obtained results show that the use of polymeric precursors in the preparation of the xerogel coatings can still well retain the hydrophobic properties of the materials. Nevertheless, both
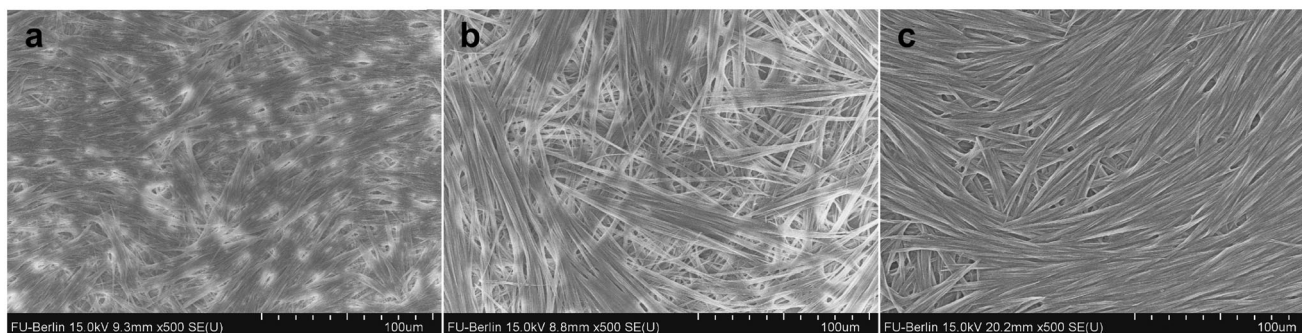
**ADVANCED
SCIENCE NEWS**

www.advancedsciencenews.com

**ADVANCED
FUNCTIONAL
MATERIALS**

www.afm-journal.de

Figure 1. SEM images of the coatings of a) **CF7** xerogel (reprinted with permission from Lee et al.[39]. Copyright 2021 American Chemical Society.), b) **CF7/PMMA** co-assembly, and c) **CF7/PTFEMA** co-assembly.

co-assemblies show drastic increases in hydrophobicity and oleophobicity compared to the polymer coatings without the fluorinated gelator (Table 1, entries 4 and 5).

Yang et al. prepared a lignin-based hydrophobic xerogel with WCA of 146°.[52] The xerogel film made from organosiloxanes by Shang et al. have WCAs up to 105°.[53] Storm et al. reported a *N*-diazeniumdiolate-modified xerogel film with WCA of 103°, which can be increased to 157° by adding nanoparticles to the coating.[54] The xerogel coatings reported in this work show similar or superior hydrophobicity and, additionally, an enhanced mechanical strength without the need for further modification.

2.3. Iterability and Durability

Aiming to fabricate coatings with improved mechanical properties, we evaluated the stabilities of the polymer-infused coating from several aspects. An enhanced mechanical stability of **CF7/PMMA** and **CF7/PTFEMA** coatings was obtained compared to that of pristine **CF7** xerogel coatings as determined by gravimetric analyses of the material loss after five water flushing cycles (Table 1 and Table S1, Supporting Information). Indeed, the presence of polymers in the coatings turns out to be

an important factor that substantially increases the mechanical stability of the materials, while maintaining their hydrophobic properties. Although the data included in this text refer to the weight percent of the material, elemental analyses of the coatings before and after water flushings suggest that these data are analogous to those referring only to weight percent of the gelator (see Table S2, Supporting Information). Thus, while the pristine **CF7** coating lost 13% of mass of the material after five water flushing cycles, these values were significantly reduced to 3.7% and 3.5% for **CF7/PMMA** and **CF7/PTFEMA** coatings, respectively (**Figure 3**a,b). The WCA has dropped to 142° ± 3° for the **CF7/PMMA** coating, and 135° ± 6° for the **CF7/PTFEMA** coating (Figure 3c,d). These values suggest that the mechanical stability of the coatings having polymers is enhanced to almost 400% compared to that of the **CF7** xerogel coating, thus compensating for the slight decrease in WCAs when coatings having improved reusability and iterability are required.

The thermal stabilities of **CF7/PMMA** and **CF7/PTFEMA** coatings were evaluated by using thermogravimetric analysis (TGA) under nitrogen stream (see Experimental Section). Pristine **CF7** and the polymers were also tested as control measurements. TGA plots show analogous thermal stabilities of
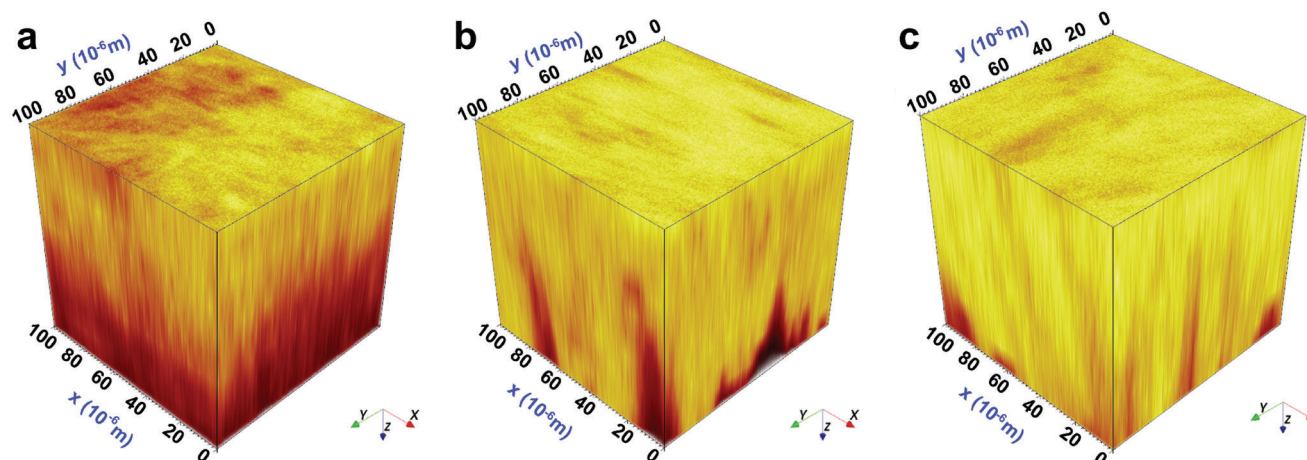

Figure 2. ToF-SIMS 3D imaging of a) **CF7** xerogel, b) **CF7/PMMA** co-assembly, and c) **CF7/PTFEMA** co-assembly. Color key: yellow = **CF7** or **CF7**-based co-assemblies; brown = glass support.

**ADVANCED
SCIENCE NEWS**

www.advancedsciencenews.com

**ADVANCED
FUNCTIONAL
MATERIALS**

www.afm-journal.de

Table 1. Characterizations of the pristine and five-times-flushed coatings.

Entry	Coating	WCA	DCA	WCA (flushed)	Material removal (flushed) [wt%]
1	**CF7**[39]	153° ± 3°	147° ± 3°	150° ± 6°	13
2	**CF7/PMMA**	149° ± 3°	85° ± 6°	142° ± 3°	3.7
3	**CF7/PTFEMA**	138° ± 4°	84° ± 2°	135° ± 6°	3.5
4	PMMA	50° ± 1°	25° ± 3°	–	–
5	PTFEMA	101° ± 3°	76° ± 3°	–	–

the pristine materials and the coatings made from the mixtures, revealing that all the samples exhibit a high thermostability upon heating to above 150°C (see Figure S10, Supporting Information).

In addition to high temperature resistance, the coatings also showed excellent frost resistance. After five cycles of freezing/defrosting, the WCAs of **CF7/PMMA** and **CF7/PTFEMA** coatings remain in the same range of the pristine materials (Figure 3e,f). These measurements together with the TGA reveal a high stability of the coatings against drastic changes in temperature.

For real-life applications, the coating can be damaged by unavoidable scratching during the process of transportation or usage. Therefore, we simulated the situation by performing scratches using a sclerometer. This test shows that the co-assemblies have a significantly higher scratch resistance. **CF7** coating is completely removed when scratching using the sclerometer with a preset force of 0.05 N, as can be observed with the eye (**Figure 4**a). In stark contrast, only a residual trace of the path of the tip of the sclerometer is shown in the optical micrographs of **CF7/PMMA** and **CF7/PTFEMA** with the above-mentioned preset force. The scratching test was repeated by increasing the force in the intervals of 0.05 N, observing that **CF7/PMMA** coating is partially removed at 2.5 N and completely removed at 2.7 N. In the case of **CF7/PTFEMA** co-assembly, these numbers decrease to 0.6 N and 0.7 N, respectively (see Figures S11 and S12, Supporting Information). Consequently, the scratch resistance is improved by a factor of 50 for **CF7/PMMA** and a factor of 12 for **CF7/PTFEMA**, compared to that of **CF7** coating. Thus, the preparation of the supramolecular-polymer co-assemblies turns out to be an effective strategy toward the improvement of the mechanical stability of the coatings, affording materials having scratch resistance properties.

2.4. Practical Implementations

We further evaluate the strength-improved hydrophobic coatings with several applications. One of the typical applications for polymer films is to prevent corrosion of the material underneath.[55–57] The co-assemblies were coated on piranha-washed copper plates, then stored in 30 mL of deionised water for 7 days. After the time period, the sample was dried and the polymeric coating was removed to expose the copper surface underneath. An uncoated copper plate was used as a control. The uncoated copper plate shows significant color change due to corrosion, while the coated samples preserve the shiny surface (Figure 4b), indicating that the co-assembly successfully functioned in corrosion prevention.

Moreover, the oleophobicity of the coatings was evaluated by dropping 100 µL of silicon oil colored with ≈2 wt% of green marker ink on the coated samples. On non-coated glass cover slips, the oil wetted the entire traveled surface. In contrast, the major fraction of the deposited oil rolled off the surface of **CF7/PMMA** and **CF7/PTFEMA** coatings, while the residue appears to be in a beaded shape or has left a much narrower trace than on the glass (Figure 4c).

3. Conclusion

While LMWGs are an easy-to-handle material for many applications, their mechanical fragility limits the potential as a coating material. The combination of LMWG with polymers can overcome this limitation and results in the development of tough and water-repellent coatings that have a broad range of applications, including industrial and biomedical applications. In our work, we have demonstrated how the formation of co-assembled coatings from **CF7** xerogels and PTFEMA or PMMA can be applied to obtain enhanced mechanical stability of the coatings. These materials were characterized using different techniques, including ToF-SIMS which allow to unambiguously confirm the uniform distribution of the polymer and the gelator in the coatings.

Interestingly, the iterability of these materials has been improved to almost 400% as a means of the water flushing resistance while retaining the hydrophobicity. Additionally, the **CF7/PMMA** and **CF7/PTFEMA** co-assemblies turn out to be significantly more scratch resistant compared to the pristine **CF7** coating. Properties of the resulting coating can be fine-tuned through the choice of the components. Future research should be focused on the combination of different LMWGs and polymers toward the preparation of co-assembled coatings having both superhydrophobicity and high mechanical and scratch resistance.

4. Experimental Section

Materials: All reagents were purchased from either abcr, Acros Organics, Apollo Scientific, Sigma-Aldrich/Merck, TCI, or VWR Chemicals. Reagents except the acrylate monomers were used directly without purification. The acrylate monomers were distilled under reduced pressure to remove the inhibitors. Menzel glass coverslips (22 mm × 22 mm × 13–16 mm) were purchased from VWR. Copper plates were acquired from the mechanic workshop of Institut für Chemie und Biochemie, Freie Universität Berlin. Both glass cover slips and copper plates were cleaned with freshly prepared piranha solution, followed by rinsing with Milli-Q water and acetone.

Sample Preparation: The organogel was prepared by dissolving 10 mg of **CF7** in the corresponding amount of diethyl ether (**Table 2**) and sonicating for 10 min. Then the corresponding amount of monomer (with 0.5 wt% of 2,2-dimethoxy-2-phenyl-acetophenone) was added to the organogel and the mixture was sonicated for another 10 min. Afterward, 5.6 µL of triethylamine was added to the mixture, and the mixture was irradiated with UVA for 20 min while stirring vigorously. 0.40 mL of the mixture was then drop-casted on a piranha-cleaned substrate, followed by UVA irradiation until dried. The coatings were further dried in a vacuum chamber overnight before any measurements or tests.

X-Ray Photoelectron Spectroscopy: XPS analysis was carried out using a SPECS EnviroESCA instrument with an excitation energy of 1486.71 eV, a detector voltage of 1650 V, and a bias voltage of 100 V.
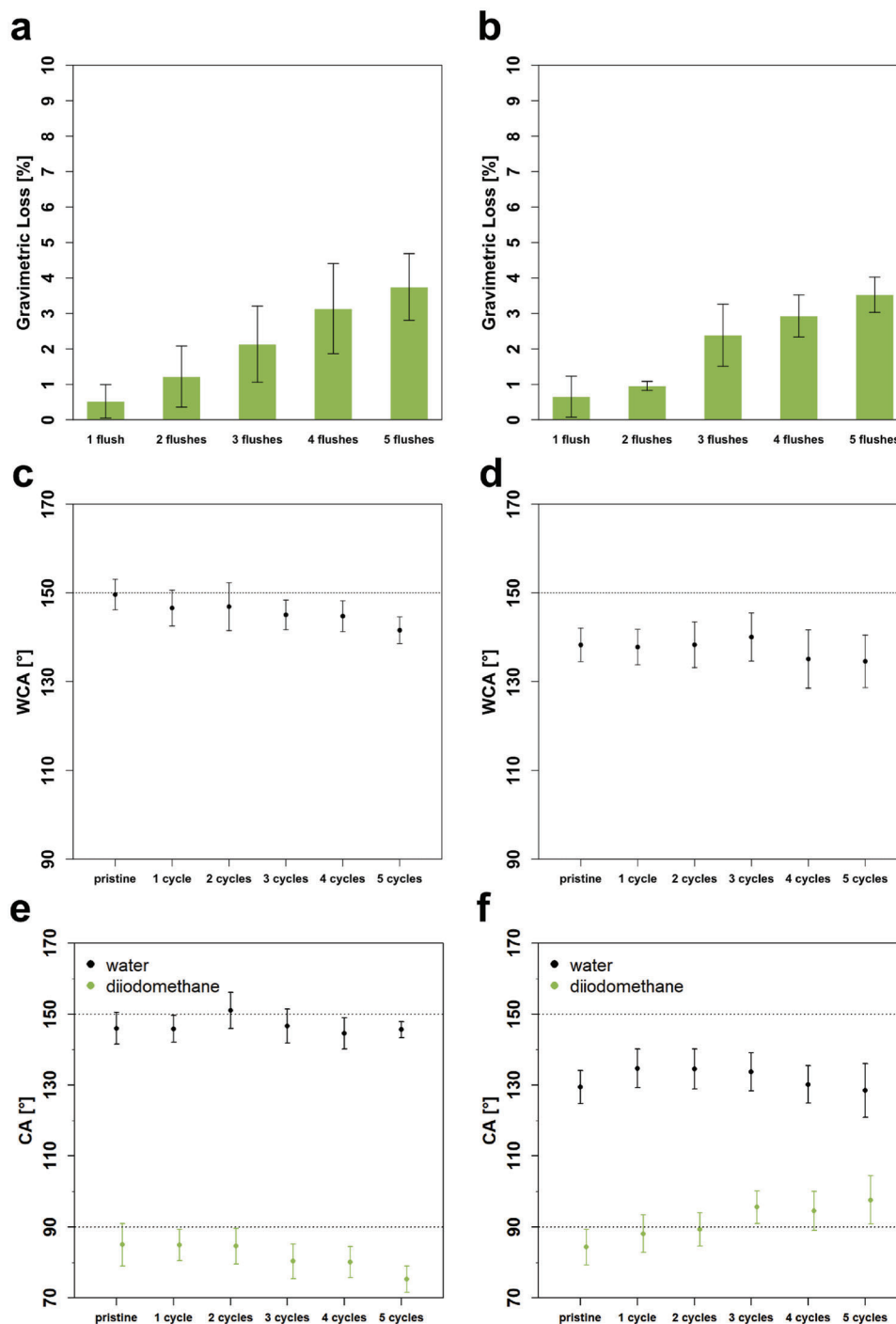
Figure 3. a) Gravimetric analyses of **CF7/PMMA** and b) **CF7/PTFEMA** coatings measured after flushing with water. c) WCAs of **CF7/PMMA** and d) **CF7/PTFMEA** coatings measured before and after flushing with water. e) WCAs and DCAs of **CF7/PMMA** and f) **CF7/PTFMEA** coatings measured before and after the freezing cycles.

Time-of-Flight Secondary Ion Mass Spectrometry: ToF-SIMS analyses were recorded using a IONTOF M6, using a Bi^{3+} primary liquid metal ion gun (LMIG) and an argon gas cluster sputter depth profiling ion gun. Sputtering was carried out by using a 20 kev Ar$_{2000}^+$ cluster ion beam. A 100 × 100 µm area was measured, repeating 30 sputtering cycles.

Thermogravimetric Analysis: Thermogravimetric analyses of the samples were recorded using a PerkinElmer TGA 8000. Measurements were performed under a nitrogen flow within the temperature range of 50–1000 °C with a heating rate of 40 °C min^{-1}. All samples were held by ceramic crucibles. Sample masses were in the range of 1–4 mg. A waiting time of 5 min was given before running the analyses with nitrogen flushing and
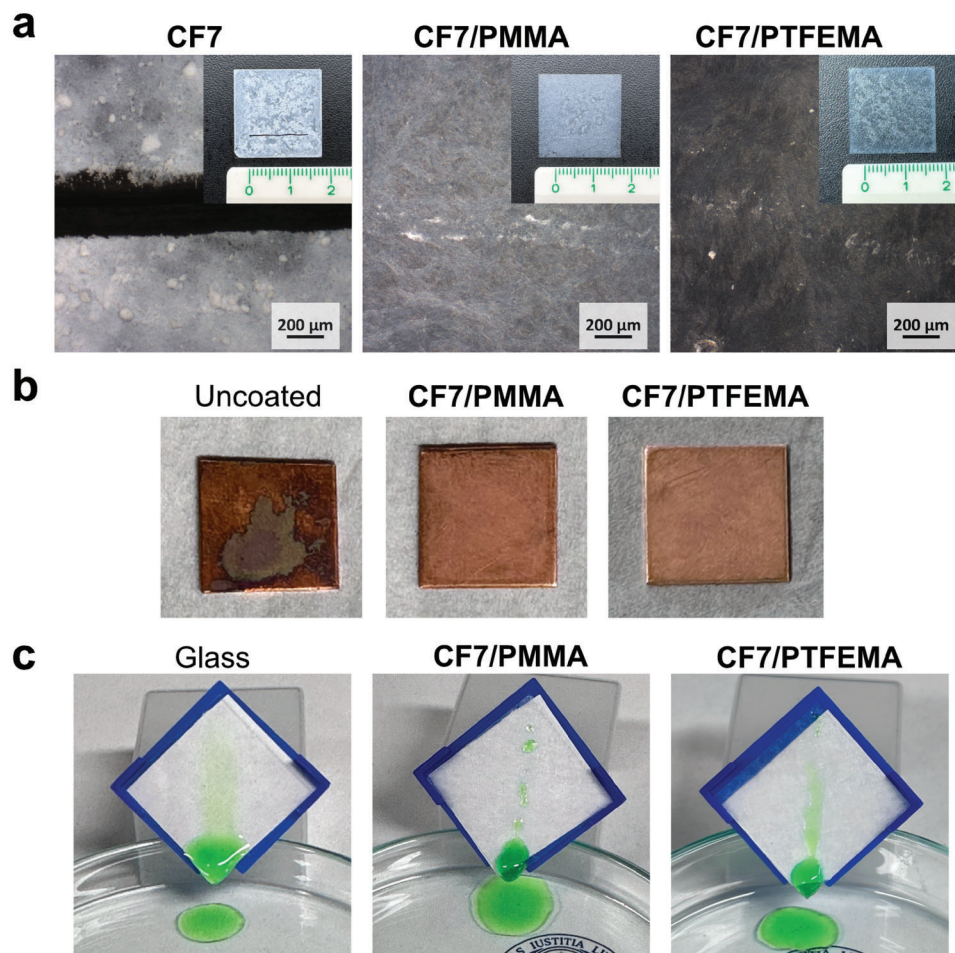
ADVANCED
SCIENCE NEWS

www.advancedsciencenews.com

ADVANCED
FUNCTIONAL
MATERIALS

www.afm-journal.de

Figure 4. a) Optical micrographs showing the scratches performed with a constant force of 0.05 N with the sclerometer. Photographs of the full length are shown in the insets. b) Copper corrosion is successfully prevented by the polymeric coatings after storing in deionised water for 7 days. c) Observed phenomena of silicon oil sliding on different surfaces.

temperature holding at 50 °C in order to ensure stable and inert conditions for all measurements.

Scanning Electron Microscopy: SEM images were conducted using a scanning electron microscope from Hitachi (SU 8030). All surfaces were precoated with a 5 nm gold layer using the sputtering system SC 500 from Emscope.

Contact Angle Measurement: All CA measurements were performed under ambient conditions using Milli-Q water or diiodomethane on horizontally placed coated substrates. The measurements were performed with a Dataphysics Contact Angle System (OCA). The analysis of the images was carried out using the software SCA 20. Laplace–Young fitting was used to determine the CA from a digital photograph of the droplet profile for static CAs, employing 3 µL of Milli-Q water (see Figure S13, Supporting Information). A set of three samples were measured to obtain nine mea-

surements (three measurements on each of the sample on random locations). The indicated average values and standard deviations were then calculated from these nine measurements, omitting the highest and lowest values. Due to the destructive note of most tests, a different set of samples were used for different characterizations.

Gravimetric Analysis: Gravimetric analyses of the coating stability were carried out on the pristine co-assembled coatings and, also, after each round of flushing on the surfaces. All rinsed surfaces were dried overnight under ambient conditions before the measurement. The indicated average values and standard deviations were calculated from three independent measurements on three different samples.

Elemental Analysis: Elemental analysis measurements were conducted using a Elementar Vario EL with two columns.

Optical Microscopy: Optical micrographs were recorded with a Zeiss Microscope Axio Scope A1 using episcopal illumination with darkfield contrasting.

Scratch Resistance: Scratch resistance measurements were tested using a TQC SP0010 sclerometer. Different preset pressures were used in an increasing sequence for testing to check the scratch resistance of the corresponding coating. The sclerometer is moved along the surface with a rate of 0.43 ± 0.2 cm s^{-1} and a total distance of 1.5 cm on every tested surface.

Frost Resistance: Frost resistance measurements were analyzed measuring the CAs after different freezing cycles. For every freezing cycle,

Table 2. The corresponding amount of solvent and monomer for the co-assemblies..

Co-assembly	Diethyl ether [mL]	Monomer [mL]
CF7/PMMA	1.1	0.90
CF7/PTFEMA	1.2	0.80

samples are placed in the freezing compartment of a standard household fridge for 2 h, then defrosted on the bench for 2 h before the measurements. Condensation disturbance from air humidity during defrosting was not observed.

Corrosion Resistance: Corrosion tests were conducted by soaking a supramolecular-polymer coated copper plate in ≈ 50 mL of deionised water for 7 days. A non-coated copper plate was used as control.

Supporting Information

Supporting Information is available from the Wiley Online Library or from the author.

Conflict of Interest

The authors declare no conflict of interest.

Data Availability Statement

The data that support the findings of this study are available from the corresponding author upon reasonable request.

[1] D. J. Abdallah, R. G. Weiss, *Adv. Mater.* **2000**, *12*, 1237.
[2] M. De Loos, B. L. Feringa, J. H. van Esch, *Eur. J. Org. Chem.* **2005**, *2005*, 3615.
[3] S. S. Babu, V. K. Praveen, A. Ajayaghosh, *Chem. Rev.* **2014**, *114*, 1973.
[4] E. R. Draper, D. J. Adams, *Chem* **2017**, *3*, 390.
[5] S. Datta, S. Bhattacharya, *Chem. Soc. Rev.* **2015**, *44*, 5596.
[6] J. Zhang, C.-Y. Su, *Coord. Chem. Rev.* **2013**, *257*, 1373.
[7] P. R. Chivers, D. K. Smith, *Nat. Rev. Mater.* **2019**, *4*, 463.
[8] S. Correa, A. K. Grosskopf, H. L. Hernandez, D. Chan, A. C. Yu, L. M. Stapleton, E. A. Appel, *Chem. Rev.* **2021**, *121*, 11385.
[9] D. Díaz Díaz, D. Kühbeck, R. J. Koopmans, *Chem. Soc. Rev.* **2011**, *40*, 427.
[10] K. Hawkins, A. K. Patterson, P. A. Clarke, D. K. Smith, *J. Am. Chem. Soc.* **2020**, *142*, 4379.
[11] M. Albino, T. J. Burden, C. C. Piras, A. C. Whitwood, I. J. Fairlamb, D. K. Smith, *ACS Sustain. Chem. Eng.* **2023**, *11*, 1678.
[12] I. Tomatsu, K. Peng, A. Kros, *Adv. Drug Deliv. Rev.* **2011**, *63*, 1257.
[13] K. J. Skilling, F. Citossi, T. D. Bradshaw, M. Ashford, B. Kellam, M. Marlow, *Soft Matter* **2014**, *10*, 237.
[14] T. Das, M. Häring, D. Haldar, D. D. Díaz, *Biomater. Sci.* **2018**, *6*, 38.
[15] D. M. Raymond, B. L. Abraham, T. Fujita, M. J. Watrous, E. S. Toriki, T. Takano, B. L. Nilsson, *ACS Appl. Bio Mater.* **2019**, *2*, 2116.
[16] C. C. Piras, A. G. Kay, P. G. Genever, D. K. Smith, *Chem. Sci.* **2021**, *12*, 3958.
[17] D. J. Cornwell, D. K. Smith, *Mater. Horiz.* **2015**, *2*, 279.
[18] M. Bielejewski, A. Rachocki, J. Kaszyńska, J. Tritt-Goc, *Phys. Chem. Chem. Phys.* **2018**, *20*, 5803.
[19] X. Cao, A. Gao, J.-T. Hou, T. Yi, *Coord. Chem. Rev.* **2021**, *434*, 213792.
[20] M. De Loos, J. van Esch, I. Stokroos, R. M. Kellogg, B. L. Feringa, *J. Am. Chem. Soc.* **1997**, *119*, 12675.
[21] M. Masuda, T. Hanada, K. Yase, T. Shimizu, *Macromolecules* **1998**, *31*, 9403.
[22] K. Inoue, Y. Ono, Y. Kanekiyo, K. Hanabusa, S. Shinkai, *Chem. Lett.* **1999**, *28*, 429.
[23] S. Kang, B. Jung, J. Chang, *Adv. Mater.* **2007**, *19*, 2780.
[24] K. Hanabusa, Y. Maesaka, M. Suzuki, M. Kimura, H. Shirai, *Chem. Lett.* **2000**, *29*, 1168.
[25] J. Sautaux, F. Marx, I. Gunkel, C. Weder, S. Schrettl, *Nat. Comm.* **2022**, *13*, 356.
[26] K. Hanabusa, A. Itoh, M. Kimura, H. Shirai, *Chem. Lett.* **1999**, *28*, 767.
[27] A. E. Way, A. B. Korpusik, T. B. Dorsey, L. E. Buerkle, H. A. von Recum, S. J. Rowan, *Macromolecules* **2014**, *47*, 1810.
[28] L. Feng, S. Li, Y. Li, H. Li, L. Zhang, J. Zhai, Y. Song, B. Liu, L. Jiang, D. Zhu, *Adv. Mater.* **2002**, *14*, 1857.
[29] H. H. Ipekci, H. H. Arkaz, M. S. Onses, M. Hancer, *Surf. Coat. Technol.* **2016**, *299*, 162.
[30] X. Huang, Y. Yuan, S. Liu, W. Wang, R. Hong, *Mater. Lett.* **2017**, *208*, 62.
[31] J. Liu, L. Ye, Y. Sun, M. Hu, F. Chen, S. Wegner, V. Mailänder, W. Steffen, M. Kappl, H.-J. Butt, *Adv. Mater.* **2020**, *32*, 1908008.
[32] R. S. Sutar, S. S. Gaikwad, S. S. Latthe, V. S. Kodag, S. B. Deshmukh, L. P. Saptal, S. R. Kulal, A. K. Bhosale, *Macromol. Symp.* **2020**, *393*, 2000116.
[33] N. Vourdas, A. Tserepi, E. Gogolides, *Nanotechnology* **2007**, *18*, 125304.
[34] M. Cardoso, V. Tribuzi, D. T. Balogh, L. Misoguti, C. R. Mendonça, *Appl. Surf. Sci.* **2011**, *257*, 3281.
[35] E. Huovinen, L. Takkunen, T. Korpela, M. Suvanto, T. T. Pakkanen, T. A. Pakkanen, *Langmuir* **2014**, *30*, 1435.
[36] K. K. Lau, J. Bico, K. B. Teo, M. Chhowalla, G. A. Amaratunga, W. I. Milne, G. H. McKinley, K. K. Gleason, *Nano Lett.* **2003**, *3*, 1701.
[37] L. Mishchenko, B. Hatton, V. Bahadur, J. A. Taylor, T. Krupenkin, J. Aizenberg, *ACS Nano* **2010**, *4*, 7699.
[38] E. K. Her, T.-J. Ko, B. Shin, H. Roh, W. Dai, W. K. Seong, H.-Y. Kim, K.-R. Lee, K. H. Oh, M.-W. Moon, *Plasma Processes Polym.* **2013**, *10*, 481.
[39] P.-W. Lee, T. Kaynak, D. Al-Sabbagh, F. Emmerling, C. A. Schalley, *Langmuir* **2021**, *37*, 14390.
[40] Q. Wei, C. Schlaich, S. Prévost, A. Schulz, C. Böttcher, M. Gradzielski, Z. Qi, R. Haag, C. A. Schalley, *Adv. Mater.* **2014**, *26*, 7358.
[41] F. Junge, P.-W. Lee, A. Kumar Singh, J. Wasternack, M. P. Pachnicz, R. Haag, C. A. Schalley, *Angew. Chem. Int. Ed.* **2023**, *62*, e202213866.
[42] H. Gankema, M. A. Hempenius, M. Möller, G. Johansson, V. Percec, *Macromol. Symp.* **1996**, *102*, 381.
[43] U. Beginn, S. Keinath, M. Möller, *Macromol. Chem. Phy.* **1998**, *199*, 2379.

**ADVANCED
SCIENCE NEWS**

www.advancedsciencenews.com

**ADVANCED
FUNCTIONAL
MATERIALS**

www.afm-journal.de

[44] U. Beginn, S. Sheiko, M. Möller, *Macromol. Chem. Phy.* **2000**, *201*, 1008.

[45] F.-X. Simon, N. S. Khelfallah, M. Schmutz, N. Díaz, P. J. Mésini, *J. Am. Chem. Soc.* **2007**, *129*, 3788.

[46] J. Stendahl, L. Li, E. Zubarev, Y.-R. Chen, S. Stupp, *Adv. Mater.* **2002**, *14*, 1540.

[47] E. Zubarev, M. Pralle, E. Sone, S. Stupp, *Adv. Mater.* **2002**, *14*, 198.

[48] V. Kostopoulos, A. Kotrotsos, S. Tsantzalis, P. Tsokanas, T. Loutas, A. Bosman, *Compos. Sci. Technol.* **2016**, *128*, 84.

[49] D. A. Stone, L. Hsu, N. R. Wheeler, E. Wilusz, W. Zukas, G. E. Wnek, L. T. J. Korley, *Soft Matter* **2011**, *7*, 2449.

[50] E. A. Wilder, K. S. Wilson, J. B. Quinn, D. Skrtic, J. M. Antonucci, *Chem. Mater.* **2005**, *17*, 2946.

[51] N. Karim, T. D. Jones, K. M. Lewandowski, B. D. Craig, S. B. Mitra, J. Yang, U.S. Patent 8,445,558 B2, **2013**.

[52] Y. Yang, Y. Deng, Z. Tong, C. Wang, *ACS Sustain. Chem. Eng.* **2014**, *2*, 1729.

[53] D. Shang, X. Sun, X. Shen, J. Hang, L. Jin, L. Shi, *Prog. Org. Coat.* **2018**, *121*, 142.

[54] W. L. Storm, J. Youn, K. P. Reighard, B. V. Worley, H. M. Lodaya, J. H. Shin, M. H. Schoenfisch, *Acta Biomater.* **2014**, *10*, 3442.

[55] R. Twite, G. Bierwagen, *Prog. Org. Coat.* **1998**, *33*, 91.

[56] S. H. Cho, S. R. White, P. V. Braun, *Adv. Mater.* **2009**, *21*, 645.

[57] D. Iqbal, J. Rechmann, A. Sarfraz, A. Altin, G. Genchev, A. Erbe, *ACS Appl. Mater. Interfaces* **2014**, *6*, 18112.